buildings

Article

Shake-Table Testing of a Cross Vault

Elizabeth Vintzileou [1,*], Charalambos Mouzakis [2], Lucia Karapitta [2] and Androniki Miltiadou-Fezans [3]

1 Laboratory of Reinforced Concrete, National Technical University of Athens, 15772 Zografou, Greece
2 Laboratory of Earthquake Engineering, National Technical University of Athens, 15772 Zografou, Greece
3 School of Architecture, National Technical University of Athens, 10682 Athens, Greece
* Correspondence: elvintz@central.ntua.gr; Tel.: +30-2107721272

Abstract: Domes, vaults and arches are structural components of high vulnerability, due to the horizontal component of the thrust they impose to the supporting vertical elements (piers or walls), accentuated by the asymmetry of loading due to seismic actions. In order to explore the possibilities of reducing this vulnerability, a cross vault made of brickwork and supported by two stone masonry walls was tested on the earthquake simulator. A series of seismic tests was performed to the specimen at its as-built state, as well as after strengthening using techniques adequate for monuments, namely, grouting of piers, arrangement of struts/ties at the base of the cross vault and vertical prestressing of the masonry piers. The tests have confirmed the vulnerability of the original specimen, as well as the improvement of its behavior after strengthening, in terms of sustained maximum base acceleration, deformations and observed damage.

Keywords: cross vault; shake-table testing; grouting; struts; ties; vertical prestressing

check for updates

Citation: Vintzileou, E.; Mouzakis, C.; Karapitta, L.; Miltiadou-Fezans, A. Shake-Table Testing of a Cross Vault. *Buildings* **2022**, *12*, 1984. https://doi.org/10.3390/buildings12111984

Academic Editors: Andreas Kappos, Leonidas Alexandros S. Kouris and André R. Barbosa

Received: 4 October 2022
Accepted: 11 November 2022
Published: 15 November 2022

1. Introduction

Arches, vaults and domes are frequently met in historical constructions and monuments, such as residential houses, churches, bridges, etc. Those elements, when subjected to vertical loads, are under axial compression. Thus, despite the low-to-medium mechanical properties of masonry, curved elements of limited thickness are able to bridge large spans. A prerequisite for the satisfactory behavior of arches and vaults is their symmetrical loading, a condition that is not satisfied in the case of seismic events. Furthermore, the curved elements transfer to their supports an inclined force. The horizontal component of the thrust causes horizontal displacements to the vertical supporting elements (piers or walls). Rather frequently, the stiffness of the vertical elements is not adequate and, thus, their significant "out-of-plomb" deformations lead to damage of arches and vaults. The problem is aggravated by the fact that the vertical elements are connected to the curved elements at their top, where the vertical loads are of small value and, thus, their out-of-plane stiffness and flexural capacity cannot take profit of a substantial beneficial vertical compression. In a significant number of monuments, precious frescoes, paintings and other decorative elements cover the interior (intrados) of a system of vaults and arches (Figure 1a). Strong earthquakes that occurred during the lifetime of the UNESCO listed Katholikon of Daphni monastery (Attica, Greece) have caused significant damage to the system of vaults and arches (Figure 1b) and to the perimeter walls, and they have led to the loss of extensive portions of the 11th century mosaics. Furthermore, the central cupola, as well as a significant portion of the perimeter walls at its west part, were reconstructed in the late 19th–early 20th century, following two strong earthquakes that occurred at the end of the 19th century [1]. The seismic vulnerability of the system of arches and vaults of the Katholikon, as well as their effect on the supporting vertical elements, are documented in situ: (a) Figure 2 shows the south wall of the church. This wall was partly reconstructed during the major intervention of the early 20th century. The original portion of the wall (towards east) has moved out of its plane, due to the effect of the system of vaults and arches. This out-of-plane deformation (exceeding 0.20 m at the top of the wall) defines the border between the original part of the wall and that which was reconstructed following the original interior dimensions of the church; (b) In recognition of this vulnerability of the monument, during the interventions of the early 20th century, two stone masonry buttresses (Figure 3) were added in the direction N–S at both sides of the north entrance to the monument, to provide added out-of-plane stiffness to the long perimeter walls of the monument. For reasons that are not sufficiently documented, such buttresses are not present against the south wall of the church.

(**a**)

(**b**)

Figure 1. (**a**) The mosaic of Pantocrator (11th century A.D.) in the cupola and (**b**) Damage in arches and cross vaults of the Katholikon (main church) of Daphni Monastery, Attica, Greece.

It should be noted that the vulnerability due to the arches and the vaults is, in this examined case, more pronounced in the N–S direction due to the smaller lateral stiffness of perimeter walls and interior piers than in the E–W direction. It is also interesting to observe another UNESCO listed monument, the Katholikon of Hosios Loukas Monastery, Boeotia, Greece (Figure 4), 11th century, where three massive stone masonry buttresses were added perpendicular to the south wall and one more in the north wall. It is to be noted that part of the north wall of the church is in contact with an earlier built church (that of Holy Mother) and, thus, no additional lateral support was feasible or needed.

Figure 2. The south wall of the Katholikon of Daphni Monastery. The border between the original wall (towards east) and the reconstructed part (towards west) is visible.

Figure 3. The Katholikon of Daphni Monastery. Observe the two stone masonry buttresses added perpendicularly to the north wall.

Figure 4. Buttresses against the south and the north walls of the Katholikon of Hosios Loukas Monastery, Boeotia, Greece.

The Katholikon of Daphni Monastery has suffered significant damage due to the Attica earthquake, 1999. Due to the importance of this major monument, the Hellenic Ministry of Culture has planned and funded a series of investigations (in situ and in laboratory). The study of the historical pathology of the monuments, the pathology due to the 1999 earthquake, as well as numerical modelling and calculations, have confirmed the seismic vulnerability of the monument due to the system of arches and vaults [1]. With the purpose of identifying adequate interventions to reduce this vulnerability and to protect the monument against future earthquakes, the decision was made to test a subassembly on the shaking table, as described in [2]. More specifically, the piers supporting the cross vault, made of three-leaf stone masonry, were grouted, whereas a steel tie was provided to the arches at their springing line. The same subassembly was later tested within an EU funded project (NIKER), with the purpose of checking the efficiency of further strengthening techniques [3], e.g., vertical prestressing of the piers. This paper presents a summary of the testing program and the experimental results, focusing on the behavior of the rehabilitated subassembly tested within the project NIKER.

2. Literature Review

A paper published in 2019 [4] provides a comprehensive review of the numerous geometries of cross vaults in heritage structures, of typical damage observed due to vertical loads, settlements and earthquakes, as well as of experimental and numerical research performed to study the behavior of cross vaults and, to a lesser degree, to investigate the effect of various intervention techniques. This review shows an increasing interest of the international engineering community on this topic, with a large number of publications after 2000. Still, as shown in [4], published test results refer mainly to the behavior of cross vaults under vertical loads, the study of their seismic behavior being dealt with in a small number of experimental campaigns. Furthermore, it is interesting to observe that, although several strengthening techniques are applied to cultural heritage structures with the purpose of reducing the vulnerability of curved elements, the supporting experimental research is quite limited [4]. In practice, traditional techniques are preferred, such as steel ties, buttresses or diaphragms at the extrados, to account for the restrictions set by the international charters for interventions to cultural heritage structures.

In a recently published work [5], a review of experimental campaigns related to cross vaults is provided. The authors ascertain the vulnerability of groin vaults to horizontal or vertical displacements of their supports, as well as the limited research dedicated to this topic, despite the in situ observed damage in numerous heritage structures. It should be noted that in several experimental campaigns small-scale specimens are tested, e.g., 1:5 [5–9], 1:10 [10,11], 1:25 [12], 1:50 [13]. In addition to scale effects that should be addressed, small dimension specimens are made of materials other than the in situ ones, e.g., 3D printed plastic blocks [5], polystyrene [9], epoxy resin [13]. Although the expected failure mode seems to be captured, the general behavior of those specimens cannot be directly extrapolated to that of real-scale structures. Furthermore, shaking table tests are reported in three publications, namely [5-at scale 1:5, 6-at scale 1:5.5, 12-at scale 1:25 and 14-at scale 1:1]. It should be noted that dynamic similitude laws are not reported to have been taken into account for small scale specimens. In [12], cross vaults, scaled to 1:25 and supported at their four corners, were subjected to uniaxial sinusoidal excitations. The cross vaults have exhibited cracks close to the crown, perpendicular to the direction of the excitation, attributed by the authors to the spreading of the vault. Nonetheless, the obtained results are considered as preliminary by the authors. In [5], the collapse mechanism of a cross vault due to in-plane shear is studied. Two of the supports of the cross vault are fixed, whereas the remaining two are free to move. Quasi-static, dynamic identification and shaking table tests were performed on a 3D printed cross vault made with plastic units in dry construction at scale 1:5. The setup used in [7] was adopted for the quasi-static tests, whereas two alternative accelerograms were used for the shaking table tests. In all tests, the movement of the supports, as well as the seismic tests, were performed parallel to the supports that were free to move. The authors comment on the similarities and the differences in the failure due to shear induced by distortion of the cross vault, depending on the type of loading (quasi-static or dynamic). In [6], a portion of a church (the Fossanova church in Priverno, Italy) was scaled to 1:5.5, and it was subjected to uniaxial seismic tests. The N-S component of the Irpinia (Calitri) earthquake was imposed in the weak direction of the subassembly, i.e., out of the plane of the masonry walls supporting the cross vaults. Cracks in the arches and the vaults, parallel to the supporting walls, were recorded, along with gradual reduction of the natural frequency of the structure for increasing seismic input. The observed damage was found to be similar to that identified through numerical calculations. Finally, in [14], uniaxial seismic tests were performed to a full-scale subassembly, along its weak direction, i.e., perpendicular to the walls supporting the cross vault. The subassembly at its as-built state exhibited an increasing in width separation of the vault from its supporting walls for increasing base acceleration, as well as a horizontal crack at the crown of the vault, parallel to the walls. The stiffening effect of a pair of inclined steel strands, positioned in the opening of one of the supporting walls, was also investigated.

The review of the available literature related to the experimental study of cross vaults shows that the experimental campaigns investigate the behavior of cross vaults under vertical loads, under differential settlements of their supports, under spreading supports, as well as under seismic actions. Nonetheless, the experimental results obtained from shake-table tests are limited in number, whereas the small scale of most of them poses the problem of scale effects that is not accounted for by the respective researchers. Furthermore, the shake-table tests on cross vaults after intervention are rather scarce, e.g., [15], whereas the use of materials in organic matrix (FRPs) are criticized from the viewpoint of the principles of interventions to heritage structures. Their drawbacks relate mainly to their detachment from the substrate at limited deformation values, and their high mechanical properties compared to the low mechanical properties of the in-situ materials are also of concern.

The state of knowledge related to the seismic behavior of cross vaults, as well as to the efficiency of various intervention techniques, has led to the experimental campaign presented herein. The key decisions related to this campaign are the following: (a) testing a subassembly as close as possible to natural scale, respecting the limitations of the earthquake simulator, with the purpose of (b) reproducing the damage observed in monuments after the occurrence of earthquakes and (c) checking the efficiency of intervention techniques that may be applied even to monuments of high importance.

3. The Specimen, the Experimental Setup, the Instrumentation

The specimen (Figure 5a) constitutes a 2:3 scaled model of a cross vault (Figure 5b) on two parallel walls (Figure 5c) [3]. The plan dimensions of the specimen are 2.70 × 2.60 m^2, while the height of the walls is equal to 2.60 m, and the overall height of the specimen equals 2.85 m. The cross vault, with a thickness at its crown equal to 0.20 m, is made of solid bricks having a mean compressive strength equal to 17 MPa and a lime-pozzolan mortar, with a mean compressive strength equal to 4.35 MPa and mean flexural strength of 1.58 MPa [16]. The walls, 450 mm thick, are made of three-leaf stone masonry (Figure 5d), following the construction typology identified in situ [17]. The exterior leaves of masonry are of average thickness equal to 192 mm (the exterior leaf) and 135 mm (the interior leaf), whereas the intermediate leaf (of average thickness 123 mm) is made of a mix of small pieces of stones and mortar, as described in detail in [16]. There are no header stones transversely connecting the exterior leaves of masonry.

The subassembly is constructed on a steel base made of HEB300 profiles, through which it is adequately fixed on the earthquake simulator for testing (Figure 6). To fix the steel base to the shake table, 36 bolts M30, quality 8.8, were used.

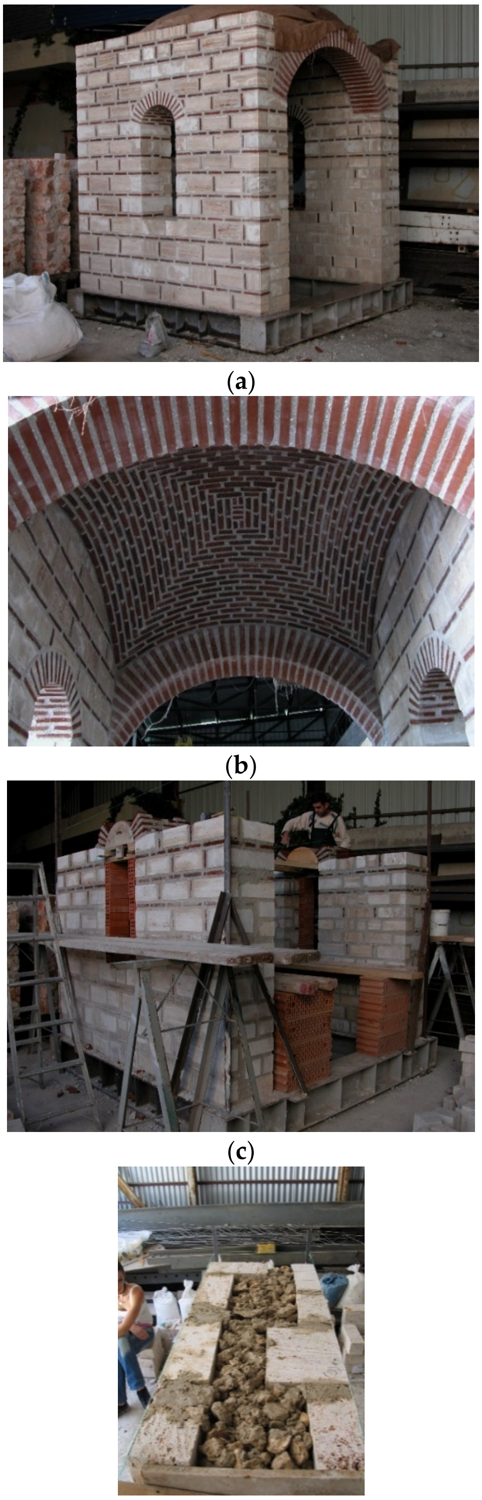

(**a**)

(**b**)

(**c**)

(**d**)

Figure 5. (**a**) The subassembly, (**b**) The cross vault (intrados) and (**c**,**d**) Construction of piers.

During testing, accelerations and displacements were continuously recorded using measuring devices (Figure 7). Accelerometers and displacement transducers were installed in critical locations, while one triaxial accelerometer was installed at the top of the cross vault throughout testing (at as-built and at strengthened state). Finally, during the last series of seismic tests, strain gauges were installed on the CFRP laminates used to provide vertical precompression to the piers, in order to measure their degree of activation.

Figure 6. The specimen on the shaking table.

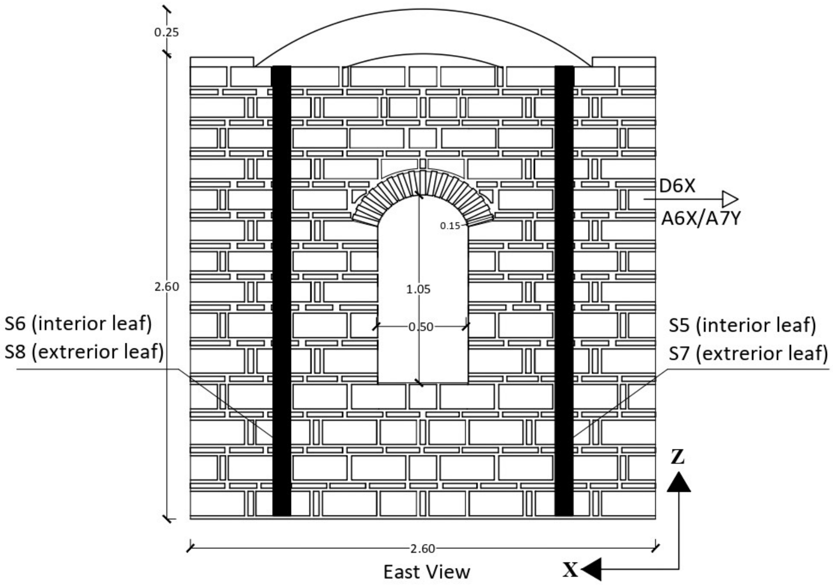

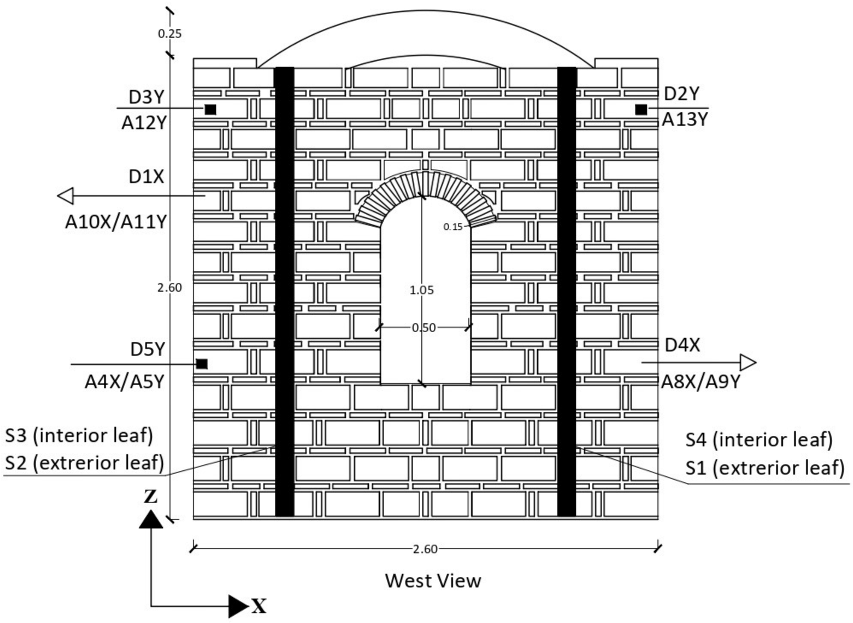

Figure 7. *Cont*.

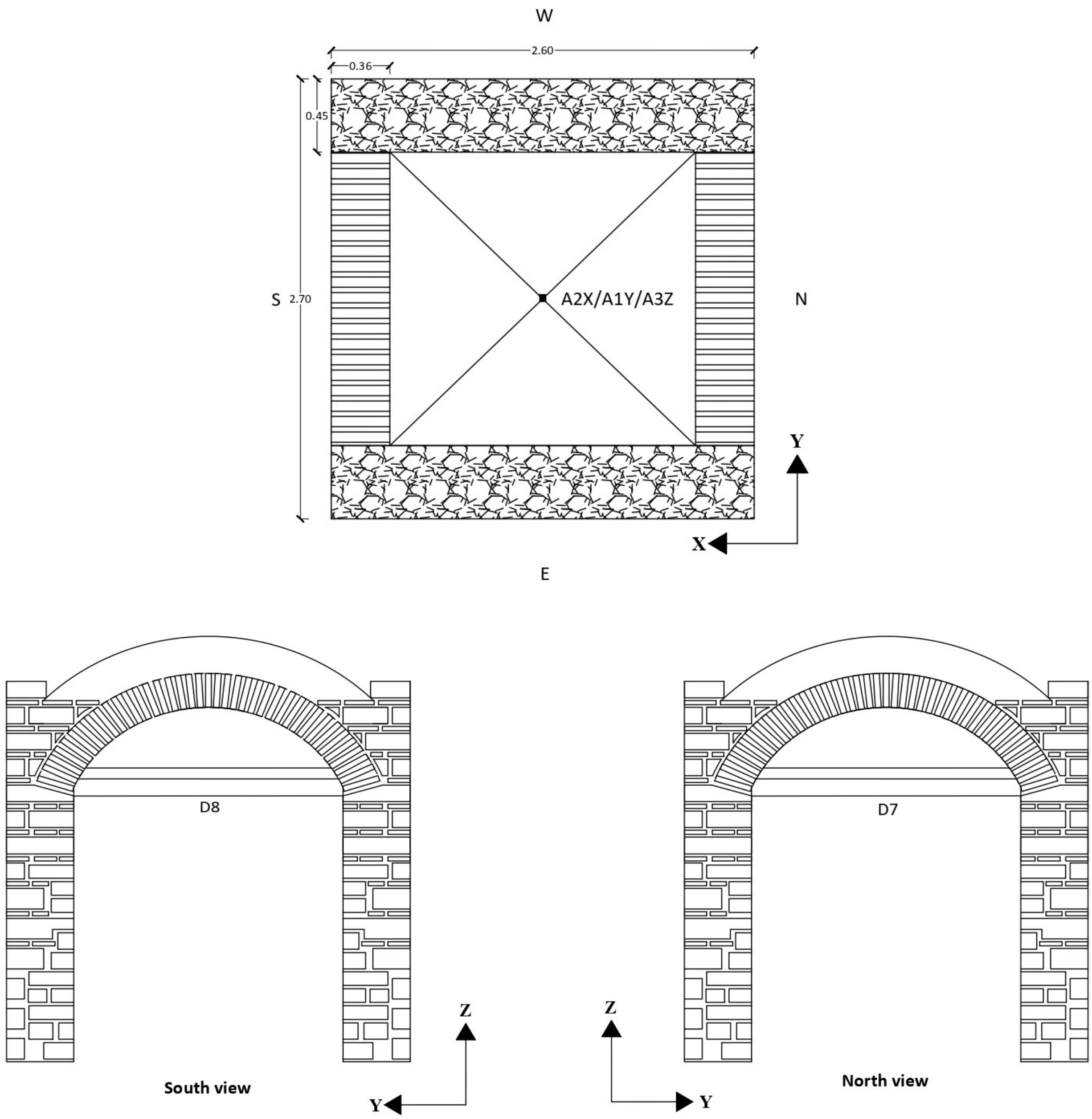

Figure 7. Instrumentation of the subassembly for the series of seismic tests within NIKER project: "A" stands for accelerometers, "D" stands for displacement transducers. Two strain gauges were installed on each CFRP plate (one per face).

4. Interventions

The as-built subassembly was subjected to a series of seismic tests that led to significant but repairable damage. This phase I is described in detail in [18]. Subsequently, the subassembly was removed from the table; the cracks occurred during phase I were injected using a hydraulic grout. In addition, two steel ties were positioned approximately at the level of the springing line of the two arches, i.e., along the E–W direction. The diameter of the steel rods was equal to 25 mm, while their yield strength was equal to 235 MPa. Then, the specimen was subjected to a series of uniaxial seismic tests, along the X direction, with the purpose of causing damage to the piers. This phase II is presented in detail in [19]. The specimen was again removed from the shake table. The stone masonry of the piers was homogenized using a hydraulic lime-based grout with a mean compressive strength, at the age of 90 days, equal to 5.3 MPa [20]. Subsequently, the subassembly was again subjected to a series of uniaxial seismic tests along the strong X direction. Cracks were caused to the piers due to in-plane shear. This phase III is described in detail in [21]. The final phase of testing, on which this work focuses, was performed within the project NIKER. After completion of phase III, the subassembly was subjected to further interventions as follows: (a) All cracks in masonry were filled using a hydraulic lime-based grout, developed within the project NIKER. The mean compressive strength of this grout, at the age of 90 days, was equal to 2.9 MPa [22]. The same grout was used to repair all cracks in the piers and the cross vault; (b) With the purpose of the interventions being to reduce the vulnerability of the cross vault along Y direction, two timber struts with incorporated steel ties (Figure 8) were installed in the north and south arches (Figures 8 and 9). The cross-sectional dimensions of the (class C30) timber ties were 100 × 100 [mm], whereas the steel ties were smooth, 25-mm diameter rods, of yield strength equal to 235 MPa. As shown in Figure 8, grooves were curved at the intrados of the arches for the accommodation of the timber struts. The struts were drilled throughout their length to allow for the positioning of the steel ties, which were anchored by means of steel plates on the east and west faces of the specimen, as shown in Figure 9. Finally, (c) vertical prestressing was imposed to the masonry piers (Figure 9) using four pairs of CFRP plates. To this purpose, the Sika® CarboDur® 624 prestressing system was used. The width of the plates is equal to 60 mm, and their thickness equals 2.6 mm. The nominal tensile strength of the plates is equal to 2800.0 MPa and the ultimate strain 1.7%. The modulus of elasticity equals 165 kN/mm^2. The plates were anchored in the steel base of the subassembly, whereas two slots were drilled in the cross vault at its junction with the piers for the accommodation of the CFRP plates. The prestressing force was equal to 100 kN per pair of plates, resulting in a vertical compressive stress on the piers equal to 0.20 MPa, roughly corresponding to the self-weight of a 10-m-high wall. It is noted that, as the prestress force is applied to a limited masonry area, the local compressive stress at the anchorage of the CFRP plates should not exceed a limiting value (selected to be 50% of the uniaxial compressive strength of masonry). As mentioned in the Introduction, one of the causes of vulnerability of the masonry elements supporting arches, vaults, etc., is due also to the limited vertical load applied to them. Indeed, as the curved elements are at the top of the structure, their self-weight constitutes practically the sole vertical load on the supporting piers. Thus, their out-of-plane flexural resistance is rather small and easily exhausted due to the horizontal component of the thrust imposed by the curved elements. Therefore, the scope of the vertical precompression was to increase the compressive stress on the piers, in order to enhance their out-of-plane flexural capacity and to, thus, postpone their damage. After the application of the interventions, the subassembly was subjected to the final series of biaxial XY seismic tests until failure.

Figure 8. Positioning of timber strut and steel tie in the arch.

Figure 9. The subassembly on the shake table; application of the vertical prestressing.

5. Performed Tests

The subassembly was subjected either to white noise tests (frequency content DC-50 Hz and constant acceleration equal to 0.02 g) or to sine sweep tests (frequency range between 1.0 Hz and 32 Hz at a rate of one octave per minute with an amplitude of 0.04 g). White noise tests were performed on the as-built subassembly, whereas sine sweep tests were performed on the strengthened specimen. Both techniques were applied separately along X and Y directions, and they provide data on the dynamic characteristics of the specimen.

Series of seismic tests were performed, with gradually increasing maximum base acceleration as described in Table 1. For the seismic tests, the signals recorded at Calitri during the 23 November 1980 Irpinia earthquake (Ms = 6.9) were used. The main characteristics of this event are: (a) its duration, approximately equal to 90 s and (b) the sequence of two main shocks of approximately equal maximum acceleration. For the tests described herein, the first part of the recorded accelerograms were used (Figure 10), namely, the E–W component was imposed along the X direction of the subassembly, while the N–S component along the Y direction. The base motion was scaled stepwise up to 150% for the subassembly at its as-built state (BS) and up to 450% for its strengthened state (AS). This motion has been found to be severely damaging to historical masonry structures and is widely used for the experimental investigation of the seismic response of such structures, both as-built and strengthened (e.g., [6,23]). Additionally, as shown in Figure 10, the spectral accelerations take their larger values in a range of 0.15 s and 1.0 s, i.e., in the range of the fundamental periods of the subassembly along both tested directions. Therefore, this ground motion was expected to lead to severe damages of the subassembly.

Table 1. Protocol of tests.

Test Name	Excitation	Direction of Excitation	Amplification of Original Record (%)
1BS	*White noise*	*X*	-
2BS	*White noise*	*Y*	-
3BS	*White noise*	*Z*	-
4BS-17BS	Irpinia	X	Gradually increasing from 30 to 500
18BS	Irpinia	XY	50
19BS	Irpinia	XY	100
20BS	Irpinia	XY	150
1AS	*Sine sweep*	*X*	-
2AS	*Sine sweep*	*Y*	-
3AS	*Sine sweep*	*X*	-
4AS	*Sine sweep*	*Y*	-
5AS	Irpinia	XY	50
6AS	Irpinia	XY	100
7AS	Irpinia	XY	150
8AS	Irpinia	XY	200
9AS	Irpinia	XY	250
10AS	Irpinia	XY	300
11AS	Irpinia	XY	350
12AS	Irpinia	XY	400
13AS	Irpinia	XY	450
14AS	*Sine sweep*	*X*	-
15AS	*Sine sweep*	*Y*	-

BS: Before Strengthening, AS: After Strengthening. 1AS and 2AS: Dynamic characteristics measured after strengthening (filling of cracks with grouting and installing struts and ties) and before the application of the vertical prestressing, 3AS and 4AS: Dynamic characteristics measured after the application of the vertical prestressing of the piers.

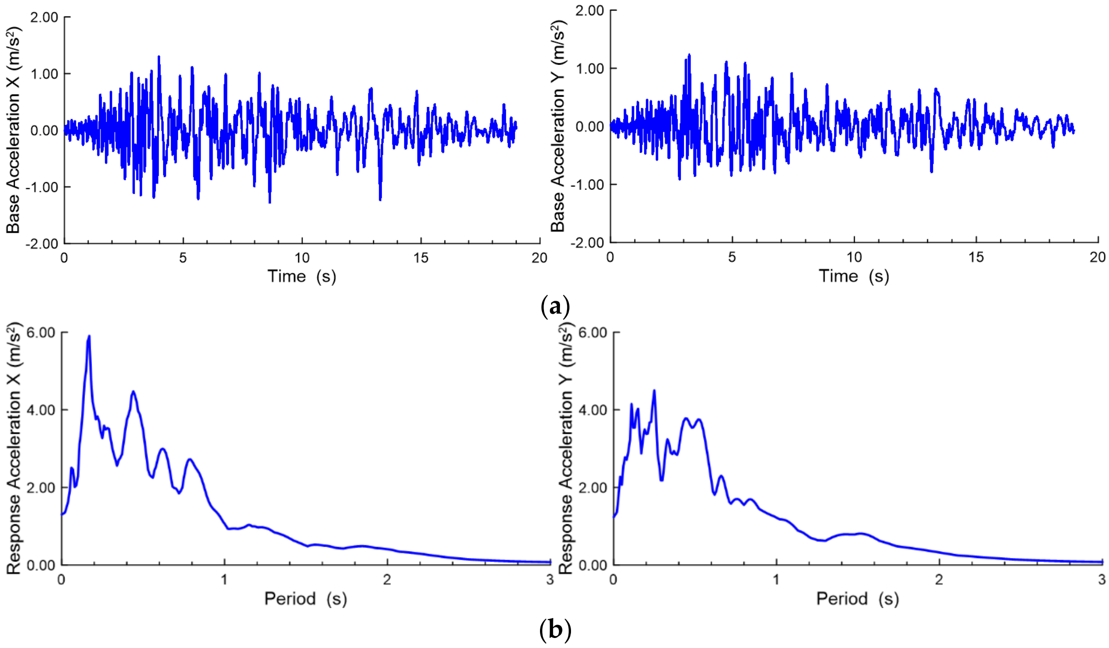

Figure 10. (**a**) The E–W and the N–S components of the Irpinia earthquake accelerograms imposed to the subassembly and (**b**) the respective response spectra for 5% damping.

6. Results

This section focuses on the experimental results obtained during the fourth and final phase of testing the subassembly. In order to assess the effect of the chosen interventions, selected experimental results from phase I are also presented herein. It should be noted that the results of phases II and III are not included in this paper, as they refer to uniaxial seismic tests in the plane of the piers supporting the cross vault. The purpose of the uniaxial tests that are not reported herein was to investigate the in-plane behavior of the piers, before and after the application of hydraulic grout. During those tests, the observed damage was limited to shear cracks in the piers and, thus, the integrity of the cross vault was not affected. Therefore, the results presented herein are those of biaxial seismic tests on the subassembly at its as-built state and at its strengthened state within NIKER program, as well as the results of the limited in number biaxial tests performed on the subassembly at its as-built state.

6.1. Dynamic Characteristics of the Subassembly

As shown in Table 1, the dynamic characteristics of the subassembly were measured at various stages of the loading history. The respective results are presented in Table 2. At all stages at which the dynamic characteristics were measured, the pronounced vulnerability of the subassembly along the Y direction is apparent, as shown by the significantly lower frequency than for X direction. The same feature was observed in shake-table tests on the building model made of unreinforced masonry [23], where the diaphragms at floor levels were flexible in their plane, and the masonry walls in one direction were longer than in the other direction. It seems that this pronounced vulnerability persists, even after on-purpose interventions (e.g., strut and tie at the spring of the arches and vertical prestressing) are applied. On the contrary, grouting of the piers and vertical prestressing seems to reinstate the original frequency along X direction, despite the damage that preceded the interventions. It should be noted that, typically, the damping ratio of the repaired and strengthened subassembly is higher than the as-built specimen. Moreover, this increase in damping ratio is more significant along the weak Y direction.

Table 2. Dynamic characteristics of the subassembly.

Test Name	Direction	Frequency (Hz)	Damping Ratio (%)
1BS	X	12.30	1.00
2BS	Y	5.96	2.00
1AS	X	10.68	3.47
2AS	Y	3.52	4.67
3AS	X	13.15	3.45
4AS	Y	4.98	4.80
14AS	X	12.38	3.48
15AS	Y	3.78	6.96

6.2. Observed Damage

During the Test 20BS, for 150% Irpinia earthquake, the subassembly has suffered significant damage, as shown in Figure 11. The cross vault was detached from the masonry piers (Figure 11a), as a result of the horizontal component of the thrust. This damage, quite similar to the damage observed in [14], led to an out-of-plomb displacement of the N–E side of the specimen by almost 15 mm (Figure 11b) at the level of the springing line of the arch. The damage to the two arches, compatible with the detachment of the cross vault from the piers, are shown in Figure 11c–f. Indeed, the arches were cracked close to their supports, in continuation of the cracks separating the cross vault from the piers. For this seismic test, the piers have exhibited slight damage, mainly sporadic horizontal cracks of small width.

Figure 11. Damage observed in the subassembly at its as-built state, after completion of biaxial seismic tests (after Test 20BS): (**a**) Detachment of the vault from the piers, (**b**) out-of-plane movement of the piers, (**c**) cracks in the arch, (**d**) separation between the vault and the pier (close up), (**e**,**f**) Detachment of the arches from the piers and cracks in the arches.

The strengthening of the subassembly using the techniques described in Section 4 did not modify the damage pattern and the mode of failure of the subassembly, as shown in Figure 12. Indeed, the cross vault was separated from the piers, whereas the arches were also severely damaged. Nonetheless, the damage, namely, the separation of the cross vault from the piers, was initiated during Test 9AS (250% Irpinia earthquake), whereas the specimen was able to sustain further seismic tests, up to 13AS (Table 1), with maximum base acceleration 4.5 times that of the original Irpinia earthquake. It should also be noted that the piers remained free of damage throughout the series of seismic tests. However, after the removal of the vertical prestressing, small opening horizontal cracks at the lower portion of the piers were observed.

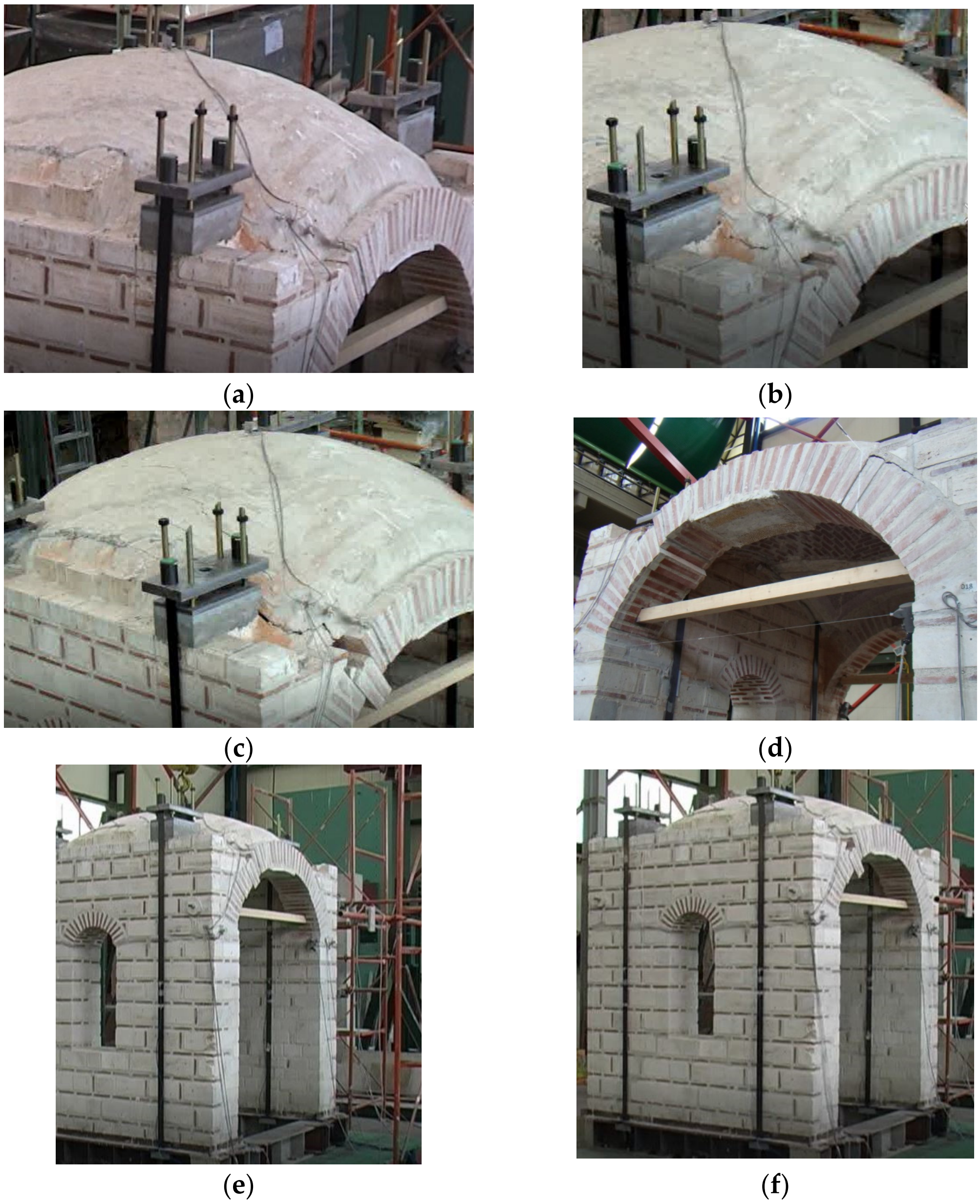

Figure 12. Development of damage to the cross vault and to the arches: (**a**) Test 11AS, (**b**) Test 12AS, (**c**) Test 13AS, (**d**) North arch, Test 13AS, (**e**) South arch, Test 12AS and (**f**) South arch, Test 13AS.

6.3. Accelerations Recorded at the Top of the Cross Vault

As shown in Figure 7, an XY accelerometer was installed at the top of the cross vault. The accelerograms recorded by this accelerometer for the final test 13AS are shown in Figure 13. The smaller period of vibration along the strong X direction of the subassembly is illustrated.

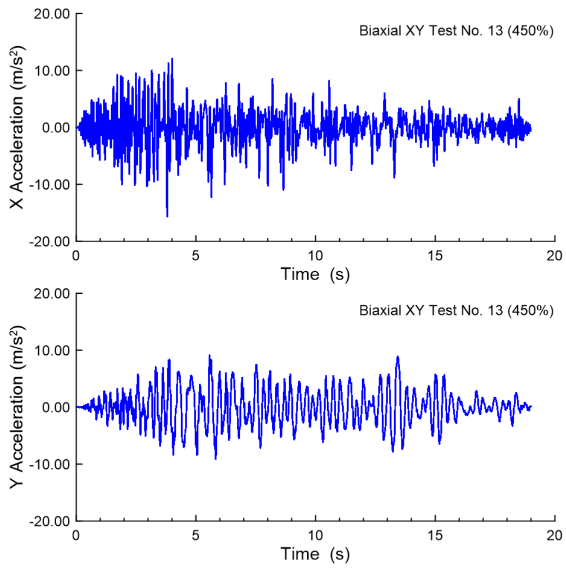

Figure 13. Accelerograms recorded at the top of the cross vault along X and Y directions, Test 13 AS.

It is interesting to observe the evolution of the maximum acceleration at the top of the cross vault as the maximum base acceleration increases (Figure 14). Along the strong direction of the subassembly, where practically no damage has occurred until the end of testing, a continuous more or less linear increase in the top acceleration is recorded. This is not the case for the weak Y direction of the subassembly, where the gradual development of damage leads to almost a plateau in the evolution of the top acceleration. In terms of maximum values of acceleration measured before and after strengthening, relevant information is provided in Table 3.

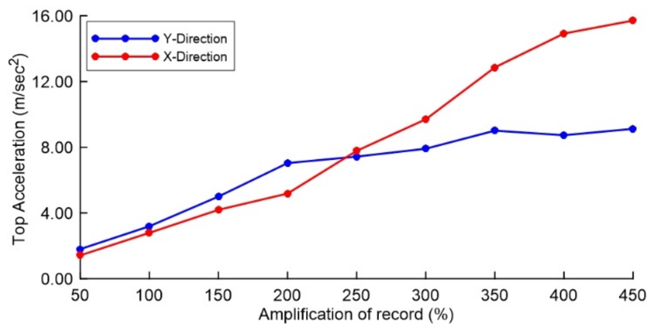

Figure 14. The evolution of the maximum acceleration measured at the top of the subassembly for the seismic tests performed after the final scheme of interventions (Tests 5AS to 13AS).

Table 3. Maximum top accelerations for the as-built and for the strengthened subassembly.

Biaxial Test XY	Base Acceleration (m/s^2)		Top Acceleration (m/s^2)	
	X	Y	X	Y
20BS (150%)	1.92	2.15	4.27	4.46
7AS (150%)	1.89	2.52	4.20	5.00
13AS (450%)	7.87	6.76	15.71	9.12

6.4. Out-of-Plane Displacements at the Top of the Piers

As shown in Figure 7, two displacement meters were installed at the top of the piers to measure the changes in their distance, i.e., their out-of-plane displacement during the seismic tests. The positive effect of the interventions, namely, the grouting of the masonry piers, the installation of a strut and a tie at the top of the piers, as well as the vertical prestressing, is depicted in the data of Table 4. Thus, the out-of-plane relative displacement of the piers, equal to 4.60 mm for the 20BS Test, is reduced to approximately 0.10 mm for the same maximum base acceleration after strengthening (Test 9AS). Even for the final test, corresponding to maximum base acceleration of 450% the Irpinia earthquake, this relative displacement did not exceed 0.25 mm in average.

Table 4. Maximum out-of-plane displacement at the top of the masonry piers.

Test Name	Maximum Out-of-Plane Displacement at the Top of the Piers (mm)
20BS (150%)	4.60 *
9AS (150%)	0.06/0.14
13AS (450%)	0.18/0.34

(*) Only one of the displacement meters gave reliable results.

It has to be admitted, though, that the relative displacement values presented in Table 4 do not seem to be in agreement with the pathological image of the subassembly, as presented in Figures 11 and 12. This is because the measurements in Table 4 refer to the level of the strut/tie at the intrados of the arches. However, there are large cracks separating the cross vault from the piers, which are not detected by those measurements. Thus, it is more appropriate to list the relative to the base out-of-plane displacements of the two piers, measured by means of the displacement meters D2Y and D3Y (Figure 7). The respective measurements are presented in Table 5. It is to be noted that the displacement meters were not located at the same height in the as-built and the after-strengthening stage of testing. In the as-built stage, the measuring devices were located at the level of the springing line of the arches, whereas at the after-strengthening stage, they were located higher up (Figure 7), as their original location coincided with the location of the strut/tie. By deliberately assuming a linear distribution of displacements along the height of the subassembly, the equivalent values for the as-built case are shown in Table 5, in parentheses. The improvement in behavior in the weak Y-direction after strengthening is apparent. Finally, for the final test, in accordance with the pathology shown in Figure 12, the out-of-plane displacement is almost three times larger than for Test 7AS.

Table 5. Relative to base out-of-plane displacements of the top of masonry piers.

Test Name	Displacement (mm)
20BS (150%)	14.83/12.52 (19.51/16.47)
7AS (150%)	7.11/17.21
13AS (450%)	34.63/39.63

6.5. Loss of Prestressing during Testing

As shown in Figure 7, the strains in the CFRP plates were measured through strain gauges. After their installation, all eight CFRP plates (in four pairs) were prestressed to the same level, ensuring an average compressive stress of 0.20 MPa in the piers. Nonetheless, as the imposed base acceleration was increasing, the out-of-plane bending moment of the two piers was also increasing. Thus, the CFRP plates located in one pier were more stressed than those located in the other pier. At the final test (13AS), an increase in the initial strain by 50% to 80% was recorded in the plates of one of the piers and a reduction by 20% to 50% in the plates of the other pier. After the completion of testing, an average loss of prestressing of 15% was recorded. In any case, the maximum stress developed in the CFRP plates did not exceed 550 MPa, a value quite small compared to the tensile strength of the plates (=2800.0 MPa).

7. Discussion

The results presented in this paper prove the efficiency of the applied intervention techniques in reducing the vulnerability of masonry arches and vaults. Nonetheless, the authors feel the need to offer several comments and self-criticism to trigger fruitful discussion with architects and engineers involved in the preservation of monuments, as well as with researchers in the same field.

The intervention techniques applied to the tested subassembly are considered to be applicable under certain conditions, even to high importance monuments, as they are either reversible or they allow for further interventions in the future. More specifically, struts and ties (a) constitute a reversible intervention that was used either in the original structure (e.g., in loggias) or as an intervention by old constructors; (b) grouting of masonry is clearly a non-reversible technique. Nonetheless, extended research has proven that when care is taken to design grouts that are fully compatible (chemically and physically) with the in situ materials, an efficient and durable intervention is ensured. Finally, (c) although the vertical prestressing of the piers is a reversible technique, it may create some concerns related to the appearance of the final result, i.e., the visible vertical plates and the quite voluminous prestressing and anchorage devices. Nonetheless, provided that there are no valuable paintings or other decorative elements on the structural elements to be prestressed, the arrangement of the prestressing "reinforcement" might be acceptable, if so needed, whereas this technique is under development and the anchorage devices may become less voluminous. Still, their anchorage at the base of the structural members to be prestressed may be questionable.

An interesting observation is that the applied intervention techniques did not alter the behavior of the structural system of the subassembly. Indeed, the damage pattern of the strengthened specimen is the same as for the as-built subassembly. Although, in principle, the preservation of the original structural system is desirable, the detachment of the cross vault from the piers and the severe damage to the arches may not be the best option, although they occur for a several times higher base acceleration than in the as-build structure. In this respect, the solution of stiffening the vaults in their plane (e.g., by providing stiff diaphragms at their extrados) and by tightly connecting those diaphragms to the vertical elements may be an effective alternative solution that deserves further investigation. This intervention, having the advantage of not being visible to the visitors, is applied to several monuments, as reported in [4,24], on the basis of meticulous numerical work. Nonetheless, the intervention is not verified and supported by experimental work. It is believed that adequate shake-table tests are needed to confirm the efficiency of the technique, to possibly reveal its drawbacks, e.g., the difficulties related to the anchorage of the stiff diaphragms to poor quality masonry and to contribute to their overcome.

A final comment is related to the testing procedure itself regarding masonry structures. The subassembly was subjected to numerous seismic tests, during several testing phases. Although, between phases, the specimen was repaired or strengthened, one has to admit that the final behavior cannot but be affected by the loading history of the subassembly. Nonetheless, as specimens such as the one tested within this work are very costly in time and in resources, typically, researchers try to take the maximum profit out of large-scale shake-table tests.

Author Contributions: E.V., PI of both research projects was responsible for the design of the specimen, she has contributed to the overall experimental work, to the evaluation of the results and to the drafting of the paper, C.M. and L.K. are responsible for the function of the shake table, they have contributed to the experimental work, to the composition of Reports and to the preparation of the publication, A.M.-F. has contributed to the design of the subassembly, to the experimental work of Phases I to III, as well as to the preaparationbof the paper. All authors have read and agreed to the published version of the manuscript.

Funding: This research was partly funded by the Hellenic Ministry of Culture in the framework of the Operational Program "CULTURE" (co-funded by the European Regional Development Fund (ERDF-75%) and by National Funds (25%)) and partly by the EU, FP7-ENV-2009-1, Contract No. 244123 (Project NIKER).

Institutional Review Board Statement: Not applicable.

Informed Consent Statement: Not applicable.

Data Availability Statement: Not applicable.

Acknowledgments: The authors wish to express their thanks to N. Delinikolas (Architect), H. Zaroyianni (Civil Engineer), S. Anagnostopoulou (Chemical Engineer), A. Kalagri (Chemical Engineer) and Ch.-E. Adami (Civil Engineer) for their contribution in various steps of this project.

Conflicts of Interest: The authors declare no conflict of interest.

References

1. Miltiadou-Fezans, A.; Vintzileou, E.; Delinikolas, N.; Zaroyianni, E.; Chorafa, E. Pathology of the Dafni Monastery: Survey, monitoring of cracks, interpretationand numerical verification. In Proceedings of the 4th International Conference on Structural Analysis of Historical Constructions, Padova, Italy, 10–13 November 2004; pp. 1285–1294.
2. Miltiadou-Fezans, A. A multidisciplinary approach for the structural Restoration of the Katholikon of Daphni Monastery in Attica Greece. Keynote Paper. In Proceedings of the 6th International Conference on Structural Analysis of Historical Constructions, Bath, UK, 2–4 July 2008; pp. 71–87.
3. Mouzakis, C.; Adami, C.-E.; Karapitta, L.; Vintzileou, E. Seismic behaviour of a rehabilitated cross-vault. In Proceedings of the 8th International Conference on Structural Analysis of Historical Constructions, Wroclaw, Poland, 15–17 October 2012.
4. Bertolesi, E.; Adam, J.M.; Rinaudo, P.; Calderon, P.A. Research and practice on masonry cross vaults-A review. *Eng. Struct.* **2019**, *180*, 67–88. [CrossRef]
5. Bianchini, N.; Mendes, N.; Calderini, C.; Candeias, P.X.; Rossi, M.; Lourenco, P. Seismic response of a small-scale masonry groin vault: Experimental investigation by performing quasi-static and shake table tests. *Bull. Earthq. Eng.* **2022**, *20*, 1739–1765. [CrossRef]
6. De Matteis, G.; Mazzolani, F.M. The Fossanova church: Seismic vulnerability assessment by numeric and physical testing. *Int. J. Archit. Herit.* **2010**, *4*, 222–245. [CrossRef]
7. Rossi, M.; Calderini, C.; Lagomarsino, S. Experimental testing of the seismic in-plane displacement capacity of masonry cross vaults through a scale model. *Bull. Earthq. Eng.* **2016**, *14*, 261–281. [CrossRef]
8. Milani, G.; Rossi, M.; Calderini, C.; Lagomarsino, S. Tilting plane tests on a small-scale masonry cross vault: Experimental results and numerical simulations through a heterogeneous approach. *Eng. Struct.* **2016**, *123*, 300–312. [CrossRef]
9. Foti, D.; Vacca, V.; Facchini, I. DEM modeling and experimental analysis of the static behavior of a dryjoints masonry cross vaults. *Constr. Build. Mater.* **2018**, *170*, 111–120. [CrossRef]
10. Shapiro, E.E. Collapse mechanisms of small-scale unreinforced masonry vaults. Master Thesis, Massachusetts Institute of Technology, Cambridge, MA, USA, 2012. Available online: http://hdl.handle.net/1721.1/72648 (accessed on 31 October 2022).
11. Rossi, M.; Barentin, C.C.; Van Mele, T.; Block, P. Experimental study on the behaviour of masonry pavilion vaults on spreading supports. *Structures* **2017**, *11*, 110–120. [CrossRef]
12. Williams, M.S.; Alejandra, A.; Victoria, L.; Yip, F. Model scale shaking table tests on masonry barrel and cross vaults. In Proceedings of the 15th World Conference on Earthquake Engineering, Lisbon, Portugal, 24–28 September 2012.
13. Mark, R.; Abel, J.F.; O'Neill, K. Photoelastic and finite-element analysis of a quadripartite vault. *Exp. Mech.* **1973**, *13*, 322–329. [CrossRef]
14. Rossi, M.; Calderini, C.; Roselli, I.; Mongelli, M.; De Gerardo, C.; Lagomarsino, S. Seismic analysis of a masonry cross vault through shaking table tests: The case study of the dey mosque in Algiers. *Earthq. Struct.* **2020**, *18*, 57–72. [CrossRef]
15. Fagone, M.; Rotunno, T.; Bati, S.B. The groin vaults of St. John Hospital in Jerusalem: An experimental analysis on a scale model. *Int. J. Archit. Herit.* **2016**, *10*, 903–918. [CrossRef]
16. Vintzileou, E.; Miltiadou-Fezans, A. Mechanical properties of three-leaf stone masonry grouted with ternary or hydraulic lime-based grouts. *Eng. Struct.* **2008**, *30*, 2265–2276. [CrossRef]
17. Palieraki, V.; Vintzileou, E.; Miltiadou-Fezans, A.; Delinikolas, N. The use of radar techniques and boroscopy in investigating old masonry: The case of Dafni Monastery. *Int. J. Archit. Herit.* **2008**, *2*, 155–186. [CrossRef]
18. Carydis, P.; Mouzakis, C.; Karapitta, L. Investigation of mechanical behavior of byzantine type of masonry with or without mosaics and evaluation of various intervention techniques-Phase I. *Technical Report LEE/NTUA.*. (In Greek)
19. Carydis, P.; Mouzakis, C.; Karapitta, L. Investigation of mechanical behavior of byzantine type of masonry with or without mosaics and evaluation of various intervention techniques-Phase II. *Technical Report LEE/NTUA*. (In Greek)

20. Miltiadou-Fezans, A.; Kalagri, A.; Kakkinou, S.; Ziagou, A.; Delinikolas, N.; Zarogianni, E.; Chorafa, E. Methodology for in situ application of hydraulic grouts on historic masonry structures. The case of the Katholikon of Dafni Monastery. In In Proceedings of the 6th International Conference on Structural Analysis of Historical Constructions, Bath, UK, 2–4 July 2008; pp. 1025–1033.
21. Carydis, P.; Mouzakis, C.; Karapitta, L. Investigation of mechanical behavior of byzantine type of masonry with or without mosaics and evaluation of various intervention techniques-Phase III. *Technical Report LEE/NTUA*.. (In Greek)
22. Badogiannis, E.; Miltiadou-Fezans, A.; Ipsilanti, E.; Dedeloudis, C.; Vintzileou, E.; Kalagri, A. Mix design and performance evaluation of grouts with superfine natural pozzolan. In Proceedings of the 8th International Conference on Structural Analysis of Historical Constructions, Wroclaw, Poland, 15–17 October 2012.
23. Vintzileou, E.; Mouzakis, C.; Adami, C.-E.; Karapitta, L. Seismic behavior of three-leaf stone masonry buildings before and after interventions: Shaking table tests on a two-storey masonry model. *Bull. Earthq. Eng.* **2015**, *13*, 3107–3133. [CrossRef]
24. Miltiadou-Fezans, A.; Vintzileou, E.; Mouzakis, C.; Dourakopoulos, J.; Giannopoulos, P.; Delinikolas, N. Structural analyses of the Katholikon of Daphni Monastery with alternative interventions improving its overall behaviour. In Proceedings of the 16th European Conference on Earthquake Engineering, Thessaloniki, Greece, 18–21 June 2018.